Journal of the American College of Cardiology Vol. 57, No. 8, 2011

Published by Elsevier Inc.
ISSN 0735-1097/$36.00
doi:10.1016/j.jacc.2010.08.648

Right Ventricular Failure Following Chronic Pressure Overload Is Associated With Reduction in Left Ventricular Mass

Evidence for Atrophic Remodeling

Maxim Hardziyenka, MD, PhD,*§ Maria E. Campian, MD,* Herre J. Reesink, MD, PhD,† Sulaiman Surie, MD,† Berto J. Bouma, MD, PhD,‡ Maarten Groenink, MD, PhD,‡ Christine A. Klemens, BSc,*§ Leander Beekman, BSc,* Carol A. Remme, MD, PhD,* Paul Bresser, MD, PhD,† Hanno L. Tan, MD, PhD*‡

Amsterdam and Utrecht, the Netherlands

Objectives We sought to study whether patients with right ventricular failure (RVF) secondary to chronic thromboembolic pulmonary hypertension (CTEPH) have reduced left ventricular (LV) mass, and whether LV mass reduction is caused by atrophy.

Background The LV in patients with CTEPH is underfilled (unloaded). LV unloading may cause atrophic remodeling that is associated with diastolic and systolic dysfunction.

Methods We studied LV mass using cardiac magnetic resonance imaging (MRI) in 36 consecutive CTEPH patients (before/after pulmonary endarterectomy [PEA]) and 11 healthy volunteers selected to match age and sex of patients. We studied whether LV atrophy is present in monocrotaline (MCT)-injected rats with RVF or controls by measuring myocyte dimensions and performing in situ hybridization.

Results At baseline, CTEPH patients with RVF had significantly lower LV free wall mass indexes than patients without RVF (35 ± 6 g/m^2 vs. 44 ± 7 g/m^2, $p = 0.007$) or volunteers (42 ± 6 g/m^2, $p = 0.006$). After PEA, LV free wall mass index increased (from 38 ± 6 g/m^2 to 44 ± 9 g/m^2, $p = 0.001$), as right ventricular (RV) ejection fraction improved (from $31 \pm 8\%$ to $56 \pm 12\%$, $p < 0.001$). Compared with controls, rats with RVF had reduced LV free wall mass and smaller LV free wall myocytes. Expression of atrial natriuretic peptide was higher, whereas that of α-myosin heavy chain and sarcoplasmic reticulum calcium ATPase-2 were lower in RVF than in controls, both in RV and LV.

Conclusions RVF in patients with CTEPH is associated with reversible reduction in LV free wall mass. In a rat model of RVF, myocyte shrinkage due to atrophic remodeling contributed to reduction in LV free wall mass.
(J Am Coll Cardiol 2011;57:921–8) © 2011 by the American College of Cardiology Foundation

Right ventricular failure (RVF) secondary to chronic pressure overload determines survival in patients with chronic thromboembolic pulmonary hypertension (CTEPH) and other forms of pulmonary arterial hypertension (PAH) (1). The mechanisms underlying the development of heart failure in these patients are not fully understood. Both right ventricular (RV) and left ventricular (LV) dysfunction occur in patients with CTEPH (2–4) and other forms of chronic PAH (5–8). This may be based on the fact that RV and LV function are closely interdependent (9). In particular, because diastolic LV peak filling rate relates directly to RV ejection fraction (7), LV diastolic filling is diminished in patients with CTEPH (3,10) and other forms of chronic PAH (6–8). This may cause LV unloading and atrophy. As the diastolic and systolic function of fully (11) or partially (12,13) unloaded LV is impaired due to atrophic remodel-

See page 929

From the *Heart Failure Research Center, Academic Medical Center, University of Amsterdam, Amsterdam, the Netherlands; †Department of Pulmonology, Academic Medical Center, University of Amsterdam, Amsterdam, the Netherlands; ‡Department of Cardiology, Academic Medical Center, University of Amsterdam, Amsterdam the Netherlands; and the §Interuniversity Cardiology Institute of the Netherlands, Utrecht, the Netherlands. Dr. Tan was supported by the Netherlands Organization for Scientific Research (NWO, grant ZonMW Vici 918.86.616). All authors have reported that they have no relationships to disclose.

Manuscript received July 20, 2010, accepted August 24, 2010.

Abbreviations and Acronyms

CTEPH = chronic thromboembolic pulmonary hypertension
IVS = interventricular septum
LV = left ventricle/ventricular
MCT = monocrotaline
MRI = magnetic resonance imaging
PAH = pulmonary arterial hypertension
PEA = pulmonary endarterectomy
RV = right ventricle/ventricular
RVF = right ventricular failure

ing (14–16), we hypothesized that LV atrophy occurs in pressure overload–associated RVF, and that it contributes to heart failure pathophysiology. The aim of the present study was to provide evidence for reduction in LV mass in CTEPH patients with RVF with the use of cardiac magnetic resonance imaging (MRI). Moreover, we sought to establish whether reduction in LV mass is caused by atrophic remodeling by studying rats in which RVF secondary to pulmonary hypertension was induced by monocrotaline (MCT) injection (17). This model is suitable to study LV remodeling, because we recently found that underfilled LV of these rats exhibits electrophysiologic changes (18) that resemble those reported in atrophic LV (19).

Methods

Clinical Study

Patients. We retrospectively studied 36 consecutive CTEPH patients who were referred for pulmonary endarterectomy (PEA), and who underwent cardiac MRI at preoperative assessment. CTEPH was diagnosed as reported previously (20). PEA was performed using standardized surgical techniques (21). Preoperatively, all patients underwent pulmonary angiography and RV catheterization. Coronary angiography was routinely performed in all patients older than 50 years of age, and in patients older than 40 years of age if they had a history of smoking. Plasma brain natriuretic peptide levels were measured in all patients, and 6-min walking distance (22) was determined in 26 patients. All patients who survived PEA were reassessed by cardiac MRI at 3 to 18 months post-PEA (median, 8 months). Eleven healthy volunteers served as controls for the RV and LV volumes and mass. Particular care was taken to match control subjects for age and sex (mean age 52 ± 10 years, 5 males). All subjects included gave written informed consent. Investigations were approved by the local institutional review board.

Determination of cardiac volumes and mass by MRI. RVF was defined as MRI-derived RV ejection fraction <45% (23). Masses of LV free wall and interventricular septum (IVS) were assessed from the stack of parallel short-axis images by manual detection of endocardial and epicardial borders on each slice; the papillary muscles were excluded from analysis of masses of LV and free wall (24) (Fig. 1). The LV free wall extends from the RV-LV junction in the anterior wall to the RV-LV junction in the inferior wall, as shown in Figure 1. Cardiac volume and mass were normalized to body surface area. Additionally, the following parameters were calculated: RV and LV end-diastolic volume indexes

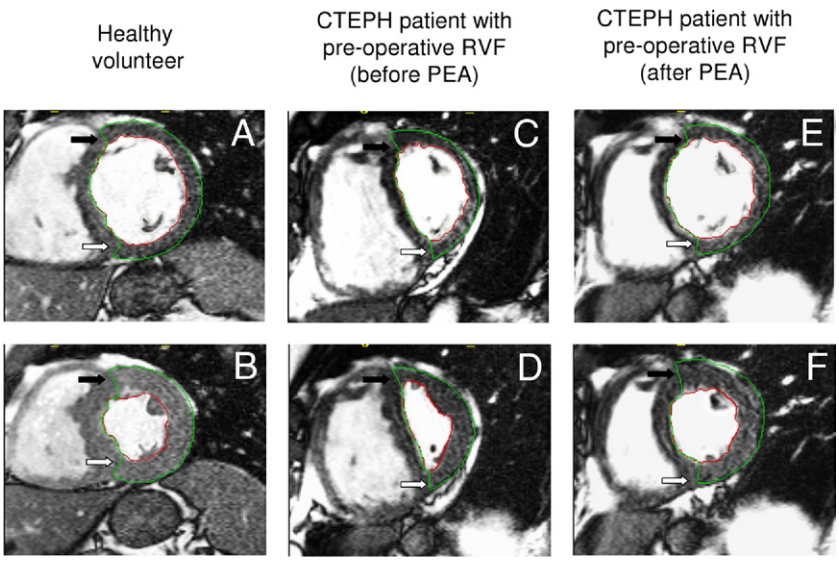

Figure 1 **Short-Axis MRI Images at the Level of Papillary Muscles**

Images from a healthy volunteer at end-diastole **(A)** and end-systole **(B)**; image from a chronic thromboembolic pulmonary hypertension (CTEPH) patient with right ventricular failure (RVF) at end-diastole **(C)** and end-systole **(D)** before pulmonary endarterectomy (PEA); images of a CTEPH patient with pre-operative RVF at end-diastole **(E)** and end-systole **(F)** after PEA. Left ventricular (LV) free wall is measured as the area encountered between manually bordered endocardial **(red)** and epicardial **(green)** curves and right ventricular (RV)-LV junction in the anterior wall (indicated with **black arrows**) to the RV-LV junction in the inferior wall (indicated with **white arrows**).

(assessment of RV and LV diastolic function); RV and LV stroke volume indexes and ejection fractions (assessment of systolic function); and LV peak filling rate (assessment of LV preload and diastolic function).

Experimental Study

Animal model. The study protocol was approved by the institutional animal use committee and was in line with European Union directives on the care and use of experimental animals. Eight-week-old male Wistar rats were injected intraperitoneally with a single dose of 60 mg/kg monocrotaline (MCT) (n = 18) to induce heart failure secondary to PAH (17). The control group (n = 18) was injected with a comparable amount (3 ml/kg) of the MCT vehicle. The animals were serially monitored clinically and by transthoracic echocardiography (17,25). MCT-injected rats and control animals were sacrificed. The heart, lungs, and liver were immediately dissected, blotted dry, and then weighed. The RV was separated from atria, IVS, and LV free wall in 10 MCT-treated animals and 10 controls, and the RV was weighed separately. Body weight and tibia length were measured (26) and used for normalization of RV, IVS, and LV free wall masses (Table 1). Hearts from MCT-injected (n = 13) and control (n = 12) animals were either enzymatically dissociated to measure cell dimensions or fixed in paraffin for in situ hybridization, or used for quantitative RT-PCR and Western blot analysis.

Statistics. The statistical analysis was performed using SPSS version 16.0 (SPSS Inc., Chicago, Illinois). Assumptions of normality and homogeneity of variance for parametric testing were assessed using the Shapiro-Wilk test. Data are mean ± SD or median with interquartile range unless otherwise indicated. Paired and unpaired Student *t* test and nonparametric Mann-Whitney *U* test were used to compare means or medians of normally and non-normally distributed values, respectively. The multiple groups were compared using 1-way analysis of variance with Bonferroni post hoc correction or Kruskal-Wallis analysis of variance by rank. Chi-square test was performed to compare proportions. $p < 0.05$ was considered statistically significant.

For detailed methods see the Online Appendix, Supplemental Methods.

Table 1 Morphometric Parameters of Rats at Sacrifice

	Control	RVF	p Value
Body weight, g	347 ± 24	279 ± 36	<0.001
Tibia length, cm	4.0 ± 0.2	3.9 ± 0.2	0.15
Lung weight, g	1.3 ± 0.1	2.3 ± 0.6	<0.001
Liver weight, g	14.7 ± 1.2	10.7 ± 1.5	<0.001
Right ventricle			
RV weight, g*	0.20 ± 0.03	0.42 ± 0.04	<0.001
RV/body weight, g/kg*	0.59 ± 0.09	1.51 ± 0.16	<0.001
RV/tibia length, g/cm*	0.05 ± 0.01	0.11 ± 0.01	<0.001
Myocyte length, μm†	107 ± 13	110 ± 8	0.70
Myocyte width, μm†	23 ± 2	27 ± 2	0.005
Left ventricle			
IVS weight, g*	0.37 ± 0.04	0.36 ± 0.02	0.42
IVS/body weight, g/kg*	1.06 ± 0.07	1.29 ± 0.16	<0.001
IVS/tibia length, g/cm*	0.09 ± 0.01	0.09 ± 0.01	0.95
Free wall weight, g*	0.68 ± 0.07	0.56 ± 0.04	<0.001
Free wall/body weight, g/kg*	1.95 ± 0.18	2.05 ± 0.34	0.42
Free wall/tibia length, g/cm*	0.17 ± 0.02	0.15 ± 0.01	0.006
Myocyte length, μm†	117 ± 8	106 ± 5	0.036
Myocyte width, μm†	25 ± 2	24 ± 1	0.58

Data are mean ± SD. n = 14 (both control and RVF) except for: *n = 6 (control) and n = 5 (RVF), and †n = 4 (control) and n = 5 (RVF) animals.
IVS = interventricular septum, LV = left ventricle; RV = right ventricle; RVF = right ventricular failure.

Results

Clinical Study

Baseline patient characteristics. On average, CTEPH patients with RVF had significantly higher mean pulmonary artery pressure and total pulmonary resistance, and significantly lower cardiac index and 6-min walking distance than patients with preserved RV systolic function (Table 2). Patients with RVF also had significantly lower LV peak filling rate and LV ejection fraction than either patients without RVF or volunteers (Table 3). No patient had coronary artery disease at coronary angiography.

LV free wall mass index in CTEPH patients with RVF. At baseline, CTEPH patients with RVF had lower LV free wall mass index than patients without RVF or volunteers. Conversely, their IVS mass index was higher than in volunteers. LV mass index was not different between the groups (Table 3). There was no significant difference between patients without RVF and volunteers with regard to RV ejection fraction, or mass indexes of LV free wall or IVS (Table 3). PEA resulted in significant improvement in RV ejection fraction (from 31 ± 8% to 56 ± 12%, $p < 0.001$) in patients with RVF at baseline (Table 4). In parallel, LV free wall mass index increased (from 38 ± 6 g/m^2 to 44 ± 9 g/m^2, $p = 0.001$), whereas IVS mass index declined (from 28 ± 8 g/m^2 to 22 ± 5 g/m^2, $p = 0.001$) compared with baseline. In contrast, patients without RVF at baseline exhibited no significant changes in RV ejection fraction (from 54 ± 9% to 56 ± 20%, $p = 0.89$) or LV free wall mass index (from 46 ± 10 g/m^2 to 50 ± 12 g/m^2, $p = 0.21$) (Table 4).

Experimental Study

Morphometric and echocardiographic parameters. Rats with RVF had significantly reduced RV contractility (low tricuspid annular plane systolic excursion), and impaired LV early diastolic relaxation and diastolic filling (low LV early diastolic relaxation velocity E′, LV early diastolic filling velocity E, LV end-diastolic area, and LV end-diastolic diameter) (Table 5). These rats also had reduced LV free wall mass (lower LV free wall weight and LV free wall/tibia length index) (Table 1). Moreover, they had smaller LV free wall myocytes, as evidenced by diminished cell length (Table 1).

Table 2 Baseline Characteristics of Patients With Chronic Thromboembolic Pulmonary Hypertension

	All Patients (n = 36)	No RVF (n = 9)	RVF (n = 27)	p Value
Age, yrs	56 ± 14	54 ± 13	57 ± 15	1.0
Male, n	13	4	9	0.69
Systolic arterial pressure, mm Hg	128 ± 17	138 ± 14	125 ± 17	0.09
Diastolic arterial pressure, mm Hg	76 ±9	82 ± 9	75 ± 9	0.25
Mean arterial pressure, mm Hg	98 ± 12	104 ± 13	97 ± 12	0.39
6-min walking distance, m	381 (167) (n = 26)	502 (80) (n = 5)	376 (137) (n = 21)	0.001
Plasma BNP level, pmol/ml	27.2 (84.9)	2.9 (9.1)	47.8 (105)	<0.001
NYHA functional class I/II/III/IV, n	0/6/27/3	0/5/4/0	0/1/23/3	0.002
Duration of symptoms, months	28 (61)	28 (75)	26 (52)	0.58
Catheterization				
mPAP, mm Hg	48 ± 13	35 ± 9	52 ± 12	<0.001
TPR, dyne/s/cm^5	935 ± 416	653 ± 224	1,037 ± 426	0.003
RAP, mm Hg	11 ± 5	8 ± 3	12 ± 5	0.08
PCWP, mm Hg	11 ± 4	9 ± 3	12 ± 5	0.42
Cardiac index, l/min/m^2	2.2 ± 0.4	2.5 ± 0.4	2.2 ± 0.4	0.027

Data are mean ± SD or median (interquartile range). RVF was defined as magnetic resonance imaging (MRI)-derived RV ejection fraction <45% (23). BNP = brain natriuretic peptide; mPAP = mean pulmonary arterial pressure; NYHA = New York Heart Association; PCWP = pulmonary capillary wedge pressure; RAP = right atrial pressure; TPR = total pulmonary resistance; other abbreviations as in Table 1.

Regional gene expression pattern, quantitative RT-PCR, and Western blot analysis. In situ hybridization revealed an altered gene expression profile: increased expression of ANP, and reduced expression of α-MHC and SERCA2 (Fig. 2). These changes were present both in RV and LV, and they were more pronounced in RV. Similarly, SERCA2 mRNA levels appeared to be reduced in RVF ventricular tissue compared with control, but these differences were not significant (Fig. 3A). ANP mRNA expression levels showed an increase in RVF versus control tissue ($p = 0.07$). These results may be consistent with the findings from the in situ hybridization experiments (Fig. 2), with regional heterogeneity of the ANP, α-MHC, and SERCA2 transcripts within the LV precluding accurate quantification. Western blot analysis did not show a significant difference in α-MHC or SERCA2 protein expression levels between control and RVF rats, although there was a tendency towards lower SERCA2 protein levels in RVF rats (Fig. 3B).

Discussion

We found that CTEPH patients with RVF had significantly lower LV free wall mass than either patients with preserved RV contractility or volunteers. In these patients, PEA restored LV free wall mass to values comparable with

Table 3 Cardiac MRI Parameters of Chronic Thromboembolic Pulmonary Hypertension Patients and Healthy Volunteers

				p Value		
	Volunteer (n = 11)	No RVF (n = 9)	RVF (n = 27)	No RVF vs. Volunteer	RVF vs. Volunteer	RVF vs. No RVF
Heart rate, beats/min	67 ± 7	73 ± 12	77 ± 10	0.08	0.03	0.64
RV						
RVEDVI, ml/m^2	67 ± 12	64 ± 18	105 ± 29	0.79	<0.001	0.001
RVSVI, ml/m^2	39 ± 7	34 ± 9	29 ± 6	0.31	0.013	0.15
RV free wall mass index, g/m^2	23 ± 5	29 ± 9	47 ± 15	0.03	<0.001	0.005
RVEF, %	59±9	55 ± 9	30 ± 10	0.14	<0.001	<0.001
LV						
LVEDVI, ml/m^2	67 ± 15	57 ± 11	53 ± 10	0.074	0.015	0.22
LVSVI, ml/m^2	44 ± 9	36 ± 8	31 ± 6	0.16	<0.001	0.043
LVPFR, ml/s	512 ± 158	466 ± 134	248 ± 86	0.10	<0.001	<0.001
LVPFR/LVEDV, s^{-1}	4.3 ± 0.6	4.0 ± 0.7	2.5 ± 0.6	0.52	<0.001	<0.001
LV mass index, g/m^2	62 ± 10	68 ± 13	62 ± 13	0.43	0.46	0.21
IVS mass index, g/m^2	20 ± 4	24 ± 6	27 ± 7	0.16	0.038	0.16
LV free wall mass index, g/m^2	42 ± 6	44 ± 7	35 ± 6	0.34	0.006	0.007
LVEF, %	66 ± 7	65 ± 8	57 ± 9	0.68	0.014	0.051

Data are mean ± SD.
LV = left ventricle; LVEDVI = left ventricular end-diastolic volume index; LVEF = left ventricular ejection fraction; LVESVI = left ventricular stroke volume index; LVPFR = left ventricular peak filling rate; RV = right ventricle; RVEDVI = right ventricular end-diastolic volume index; RVEF = right ventricular ejection fraction; RVSVI = right ventricular stroke volume index; other abbreviations as in Table 1.

Table 4 Cardiac MRI Parameters of Chronic Thromboembolic Pulmonary Hypertension Patients at Follow-Up

	No RVF* (n=4)			RVF* (n = 16)		
	Baseline	Follow-Up	p Value	Baseline	Follow-Up	p Value
Heart rate, beats/min	68 ± 11	79 ± 12	0.023	75 ± 9	76 ± 9	0.39
RV						
RVEDVI, ml/m^2	66 ± 17	54 ± 12	0.038	100 ± 25	69 ± 13	<0.001
RVSVI, ml/m^2	33 ± 7	35 ± 8	0.5	30 ± 6	37 ± 8	0.006
RV free wall mass index, g/m^2	34 ± 10	23 ± 8	0.026	47 ± 12	25 ± 5	<0.001
RVEF, %	54 ± 9	56 ± 20	0.89	31 ± 8	56 ± 12	<0.001
LV						
LVEDVI, ml/m^2	56 ± 15	53 ± 10	0.60	54 ± 10	61 ± 10	0.009
LVSVI, ml/m^2	34 ± 9	36 ± 9	0.58	31 ± 6	41 ± 9	<0.001
LVPFR, ml/s	417 ± 133	460 ± 117	0.23	252 ± 71	481 ± 141	<0.001
LVPFR/LVEDV, s^{-1}	4.0 ± 0.7	4.6 ± 0.9	0.14	2.3 ± 0.8	4.0 ± 0.7	<0.001
LV mass index, g/m^2	72 ± 17	74 ± 17	0.69	66 ± 13	66 ± 13	0.87
IVS mass index, g/m^2	26 ± 7	25 ± 6	0.46	28 ± 8	22 ± 5	0.001
LV free wall mass index, g/m^2	46 ± 10	50 ± 12	0.21	38 ± 6	44 ± 9	0.001
LVEF, %	61 ± 7	68 ± 10	0.3	58 ± 9	66 ± 6	0.003

Data are mean ± SD. *Patients indicated in the table as "no RVF" or "RVF" did not or did have RVF at baseline.
Abbreviations as in Tables 1 and 3.

volunteers. Using a rat model of RVF secondary to PAH, we found that reduction in LV free wall mass can be, at least in part, explained by myocyte shrinkage due to atrophic remodeling.

LV mass in RVF due to chronic pressure overload. In line with previous studies (10), we found that the sum of LV free wall mass index and IVS mass index was not significantly different between patients (either with or without RVF) and controls (10). However, separate analysis of IVS and LV free wall masses revealed that LV free wall mass was significantly reduced, whereas IVS was hypertrophic, in patients with RVF. We reasoned that LV free wall mass is a better reflection of LV remodeling than IVS, because IVS is composed of both LV and RV, and IVS hypertrophy may be largely explained by RV hypertrophy (10). Thus, our findings support the hypothesis that LV atrophic remodeling occurs in RVF. Accordingly, reduction in LV mass was also reported in end-stage pulmonary emphysema, another disorder that is associated with chronic RV pressure overload, dysfunction, and altered LV diastolic filling (27,28). In the present study, reduction in LV free wall volume (mass) of patients with RVF may have been underestimated because LV interstitial edema was also present (29). Interestingly, in patients with mitral stenosis (30) and end-stage pulmonary emphysema (31), disorders that are both associated with reduced LV pre-load, normalization of RV

Table 5 Echocardiographic Parameters of Rats at Sacrifice

	Control (n = 14)	RVF (n = 14)	p Value
Right ventricle			
Free-wall thickness, mm	0.7 ± 0.03	0.9 ± 0.1	<0.001
End-diastolic diameter, mm	4.1 ± 0.2	6.4 ± 0.9	<0.001
Tricuspid annulus plane systolic excursion, mm	2.2 ± 0.2	1.3 ± 0.2	<0.001
Systolic RV-RA pressure gradient, mm Hg	Not measurable (no tricuspid regurgitation)	69 ± 9	
Left ventricle			
IVS thickness, mm	1.2 ± 0.1	1.2 ± 0.2	0.14
Posterior wall thickness, mm	1.2 ± 0.1	1.3 ± 0.1	0.08
Diastolic function			
End-diastolic diameter, mm	7.5 ± 0.3	5.6 ± 0.3	<0.001
End-diastolic area, cm^2	0.67 ± 0.03	0.53 ± 0.04	<0.001
Early diastolic filling velocity (E), m/s	0.8 ± 0.1	0.6 ± 0.1	<0.001
Early diastolic relaxation velocity (E′), m/s	0.07 ± 0.01	0.04 ± 0.01	<0.001
E/E′ ratio	11.9 ± 1.5	13.5 ± 1.5	0.027
Systolic function			
End-systolic area, cm^2	0.24 ± 0.02	0.23 ± 0.02	0.1
Fractional area change,%	63.7 ± 3.0	56.5 ± 4.3	<0.001
Ejection fraction, %	68.0 ± 4.8	64.0 ± 6.9	0.15

Data are mean ± SD.
RV-RA = right ventricle-right atrium; other abbreviations as in Table 1.

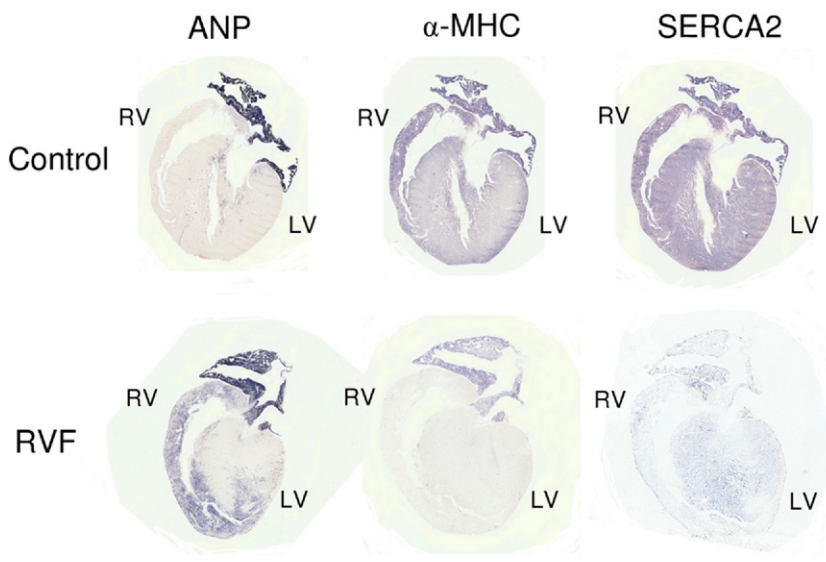

Figure 2 **Distribution of ANP, α-MHC, and sSERCA2 in a 4-Chamber Section of Control and RVF Rats**

In RVF rats **(lower panels)**, expression of ANP mRNA is higher and expression of α-MHC and SERCA2 mRNA is lower than in controls **(upper panels)**. This occurs not only in the right ventricle (RV), but also in the left ventricle (LV). ANP = atrial natriuretic peptide; α-MHC = α-myosin heavy chain; RVF = right ventricular failure; SERCA2 = sarcoplasmic reticulum calcium ATPase-2.

function and LV diastolic filling after mitral valvuloplasty and orthotopic single-lung transplantation, respectively, led to significant increase in LV mass.

In the rat model, absolute LV free wall mass in rats with RVF was significantly lower than in controls. When we normalized LV free wall weight to body weight, we found no significant difference between RVF animals and controls, in line with several previous studies, using a similar model of heart failure that described unchanged (32) or augmented (33) LV mass. However, the body weight of MCT rats declines significantly as early as 3 to 7 days prior to overt heart failure (17). Accordingly, normalization of LV mass to tibia length may be a more accurate method to reveal changes in LV mass in rats (26). This analysis showed that LV free wall mass in RVF rats was reduced. Similarly, reduction in absolute LV mass in MCT-treated rats with heart failure and rats with pulmonary artery banding was reported by other investigators (34).

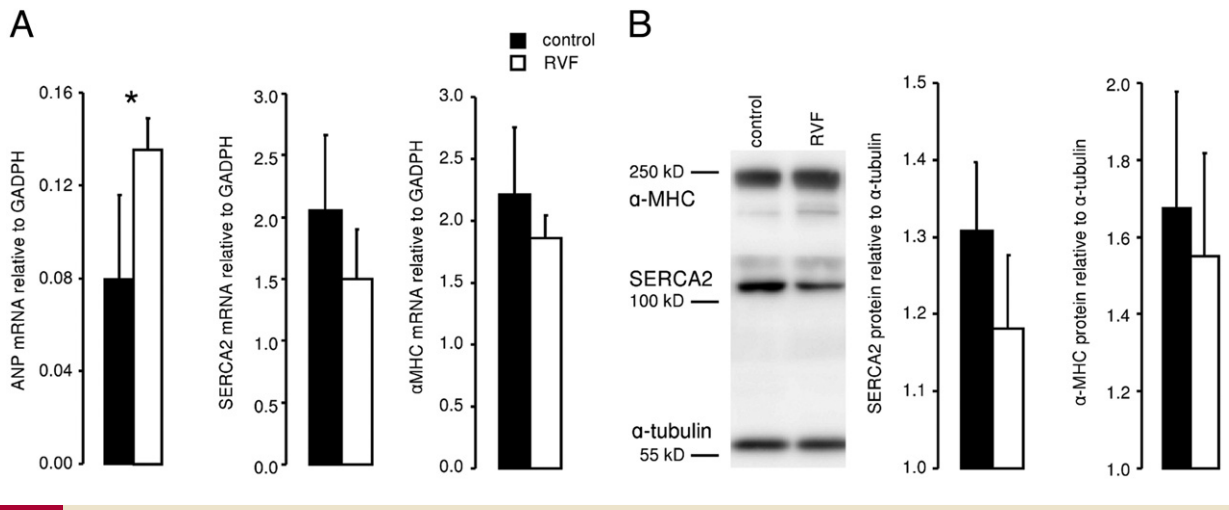

Figure 3 **mRNA Expression Levels and Western Blot Analysis of Protein**

(A) mRNA expression levels of ANP, SERCA2, and α-MHC and **(B)** Western blot analysis of SERCA2 and α-MHC with α-tubulin as loading control, in left ventricular tissue of control and RVF; data are mean ± SEM; *p = 0.07 versus control. Abbreviations as in Figure 2.

Possible mechanisms of reduction in LV free wall mass during RVF secondary to chronic PAH. Mechanical load plays a critical role in determining the mass of cardiac myocytes (35). Accordingly, unloaded LV undergoes atrophy (16,36). While doing so, it replicates the fetal gene expression profile also seen in hypertrophy (15). In the present study, we did not find LV hypertrophy. In contrast, LV mass was reduced in rats with RVF. This was associated with LV myocyte shrinkage, increased ANP mRNA expression, and diminished α-MHC and SERCA2 mRNA expression. Such a fetal gene expression profile was previously observed in the LV of MCT rats (33,37), and rats that developed RVF after chronic pulmonary artery banding (38). Of note, these changes in expressions of ANP, α-MHC, and SERCA were not predominant in the LV. Not surprisingly, they were more prominent in pressure-overloaded RV, in line with previous studies (33,38). Furthermore, although we found a similar trend in the difference in gene expression in LV between control and RVF rats using quantitative reverse transcriptase PCR (RT-PCR), Western blot analysis did not reveal significant differences in protein expression levels of α-MHC and SERCA2. Since, in the present study, LV samples for quantitative RT-PCR were taken separately from LV samples for Western blot analysis, this discrepancy may be explained by regional heterogeneity in the expression of fetal genes in myocardium of the LV in RVF (38). Taken together, these findings indicate that LV remodeling that occurs in RVF due to chronic pulmonary hypertension may be explained by cardiac myocyte atrophy (14–16,36,39). Similarly, LV myocyte atrophy was demonstrated in patients with end-stage pulmonary emphysema (27,28). Of note, myocyte atrophy is independent of catecholamines from LV tissue and/or systemic circulation, or neural activity (39,40). Although apoptosis and/or other mechanisms may also be responsible for the loss of myocardial mass in unloaded LV, atrophy may be the main mechanism (41). In line with this notion, we did not find enhanced cell death in LV free wall of MCT-treated rats with RVF (42).

Study limitations. Possible limitations of the present study are as follows. First, the number of patients studied both at baseline and at postoperative follow-up was limited. Second, cardiac MRI was performed at different time points of follow-up after PEA (ranging from 3 to 18 months with a median at 8 months). This may be important because full restoration of RV and LV systolic function after PEA requires >12 months (43). However, significant improvements in RV ejection fraction, LV end-diastolic volume, and cardiac index were documented as early as at discharge from the hospital, with further improvements being reported at 3 and 12 months of follow-up (43). Similarly, orthotopic single-lung transplantation in patients with end-stage emphysema resulted in significant improvement in RV ejection fraction and increases in LV end-diastolic volumes, stroke volumes, and LV mass as early as 3 months after surgery (31). Third, LV myocardial biopsies were not taken to assess the morphology and confirm atrophic remodeling. On the other hand, we demonstrated LV remodeling in a rat model of RVF due to chronic RV pressure overload. Although the data should be cautiously extrapolated to human disease, this experimental model is a generally accepted model to study RVF due to chronic pressure overload (17,32,44).

Conclusions

RVF in patients with CTEPH is associated with reduction in LV free wall mass. This reduction is reversible and can be restored after PEA. Using a rat model of RVF secondary to PAH, we found that reduction in LV free wall mass can be, at least in part, explained by myocyte shrinkage due to atrophic remodeling.

Reprint requests and correspondence: Dr. Hanno L. Tan, Department of Cardiology, Academic Medical Center, Meibergdreef 9, 1105 AZ Amsterdam, the Netherlands. E-mail: h.l.tan@amc.nl.

REFERENCES

1. Fedullo PF, Auger WR, Kerr KM, Kim NH. Chronic thromboembolic pulmonary hypertension. Semin Respir Crit Care Med 2003;24:273–86.
2. Chin KM, Kim NH, Rubin LJ. The right ventricle in pulmonary hypertension. Coron Artery Dis 2005;16:13–8.
3. Gurudevan SV, Malouf PJ, Auger WR, et al. Abnormal left ventricular diastolic filling in chronic thromboembolic pulmonary hypertension: true diastolic dysfunction or left ventricular underfilling? J Am Coll Cardiol 2007;49:1334–9.
4. Menzel T, Wagner S, Kramm T, et al. Pathophysiology of impaired right and left ventricular function in chronic embolic pulmonary hypertension: changes after pulmonary thromboendarterectomy. Chest 2000;118:897–903.
5. Dong SJ, Crawley AP, MacGregor JH, et al. Regional left ventricular systolic function in relation to the cavity geometry in patients with chronic right ventricular pressure overload. A three-dimensional tagged magnetic resonance imaging study. Circulation 1995;91:2359–70.
6. Krayenbuehl HP, Turina J, Hess O. Left ventricular function in chronic pulmonary hypertension. Am J Cardiol 1978;41:1150–8.
7. Lazar JM, Flores AR, Grandis DJ, Orie JE, Schulman DS. Effects of chronic right ventricular pressure overload on left ventricular diastolic function. Am J Cardiol 1993;72:1179–82.
8. Marcus JT, Vonk Noordegraaf A, Roeleveld RJ, et al. Impaired left ventricular filling due to right ventricular pressure overload in primary pulmonary hypertension: noninvasive monitoring using MRI. Chest 2001;119:1761–5.
9. Santamore WP, Dell'Italia LJ. Ventricular interdependence: significant left ventricular contributions to right ventricular systolic function. Prog Cardiovasc Dis 1998;40:289–308.
10. Reesink HJ, Marcus JT, Tulevski, II, et al. Reverse right ventricular remodeling after pulmonary endarterectomy in patients with chronic thromboembolic pulmonary hypertension: utility of magnetic resonance imaging to demonstrate restoration of the right ventricle. J Thorac Cardiovasc Surg 2007;133:58–64.
11. Ito K, Nakayama M, Hasan F, Yan X, Schneider MD, Lorell BH. Contractile reserve and calcium regulation are depressed in myocytes from chronically unloaded hearts. Circulation 2003;107:1176–82.
12. Dorfman TA, Rosen BD, Perhonen MA, et al. Diastolic suction is impaired by bed rest: MRI tagging studies of diastolic untwisting. J Appl Physiol 2008;104:1037–44.
13. Perhonen MA, Zuckerman JH, Levine BD. Deterioration of left ventricular chamber performance after bed rest: "cardiovascular deconditioning" or hypovolemia? Circulation 2001;103:1851–7.

14. Campbell SE, Korecky B, Rakusan K. Remodeling of myocyte dimensions in hypertrophic and atrophic rat hearts. Circ Res 1991;68: 984–96.
15. Depre C, Shipley GL, Chen W, et al. Unloaded heart in vivo replicates fetal gene expression of cardiac hypertrophy. Nat Med 1998;4:1269–75.
16. Klein I, Ojamaa K, Samarel AM, Welikson R, Hong C. Hemodynamic regulation of myosin heavy chain gene expression. Studies in the transplanted rat heart. J Clin Invest 1992;89:68–73.
17. Hardziyenka M, Campian ME, de Bruin-Bon HA, Michel MC, Tan HL. Sequence of echocardiographic changes during development of right ventricular failure in rat. J Am Soc Echocardiogr 2006;19: 1272–9.
18. Hardziyenka M CM, Tan HL. Right ventricular failure: electrophysiological remodeling in right ventricle precedes clinical signs (abstract). Heart Rhythm 2007;4:S173–4.
19. Schwoerer AP, Melnychenko I, Goltz D, et al. Unloaded rat hearts in vivo express a hypertrophic phenotype of cardiac repolarization. J Mol Cell Cardiol 2008;45:633–41.
20. Auger WR, Fedullo PF, Moser KM, Buchbinder M, Peterson KL. Chronic major-vessel thromboembolic pulmonary artery obstruction: appearance at angiography. Radiology 1992;182:393–8.
21. Moser KM, Daily PO, Peterson K, et al. Thromboendarterectomy for chronic, major-vessel thromboembolic pulmonary hypertension. Immediate and long-term results in 42 patients. Ann Intern Med 1987;107:560–5.
22. Reesink HJ, van der Plas MN, Verhey NE, van Steenwijk RP, Kloek JJ, Bresser P. Six-minute walk distance as parameter of functional outcome after pulmonary endarterectomy for chronic thromboembolic pulmonary hypertension. J Thorac Cardiovasc Surg 2007;133:510–6.
23. Haddad F, Hunt SA, Rosenthal DN, Murphy DJ. Right ventricular function in cardiovascular disease, part I: anatomy, physiology, aging, and functional assessment of the right ventricle. Circulation 2008;117: 1436–48.
24. Lorenz CH, Walker ES, Morgan VL, Klein SS, Graham TP Jr. Normal human right and left ventricular mass, systolic function, and gender differences by cine magnetic resonance imaging. J Cardiovasc Magn Reson 1999;1:7–21.
25. Brown L, Fenning A, Chan V, et al. Echocardiographic assessment of cardiac structure and function in rats. Heart Lung Circ 2002;11:167–73.
26. Yin FC, Spurgeon HA, Rakusan K, Weisfeldt ML, Lakatta EG. Use of tibial length to quantify cardiac hypertrophy: application in the aging rat. Am J Physiol 1982;243:H941–7.
27. Foraker AG, Bedrossian CW, Anderson AE Jr. Myocardial dimensions and proportions in pulmonary emphysema. Arch Pathol 1970; 90:344–7.
28. Sutinen S, Paakko P, Tienari J. Weights of the body and cardiac ventricles in pulmonary emphysema. Virchows Arch A Pathol Anat Histopathol 1985;407:249–57.
29. Laine GA, Allen SJ. Left ventricular myocardial edema. Lymph flow, interstitial fibrosis, and cardiac function. Circ Res 1991;68:1713–21.
30. Tischler MD, Sutton MS, Bittl JA, Parker JD. Effects of percutaneous mitral valvuloplasty on left ventricular mass and volume. Am J Cardiol 1991;68:940–4.
31. Rensing BJ, McDougall JC, Breen JF, Vigneswaran WT, McGregor CG, Rumberger JA. Right and left ventricular remodeling after orthotopic single lung transplantation for end-stage emphysema. J Heart Lung Transplant 1997;16:926–33.
32. Lamberts RR, Vaessen RJ, Westerhof N, Stienen GJ. Right ventricular hypertrophy causes impairment of left ventricular diastolic function in the rat. Basic Res Cardiol 2007;102:19–27.
33. Usui S, Yao A, Hatano M, et al. Upregulated neurohumoral factors are associated with left ventricular remodeling and poor prognosis in rats with monocrotaline-induced pulmonary arterial hypertension. Circ J 2006;70:1208–15.
34. Werchan PM, Summer WR, Gerdes AM, McDonough KH. Right ventricular performance after monocrotaline-induced pulmonary hypertension. Am J Physiol 1989;256:H1328–36.
35. Sadoshima J, Izumo S. The cellular and molecular response of cardiac myocytes to mechanical stress. Annu Rev Physiol 1997;59:551–71.
36. Kolar F, MacNaughton C, Papousek F, Korecky B, Rakusan K. Changes in calcium handling in atrophic heterotopically isotransplanted rat hearts. Basic Res Cardiol 1995;90:475–81.
37. Ishikawa S, Honda M, Yamada S, et al. Different biventricular remodelling of myosin and collagen in pulmonary hypertension. Clin Exp Pharmacol Physiol 1992;19:723–32.
38. LekanneDeprez RH, van den Hoff MJ, de Boer PA, et al. Changing patterns of gene expression in the pulmonary trunk-banded rat heart. J Mol Cell Cardiol 1998;30:1877–88.
39. Geenen DL, Malhotra A, Buttrick PM, Scheuer J. Increased heart rate prevents the isomyosin shift after cardiac transplantation in the rat. Circ Res 1992;70:554–8.
40. Lisy O, Redfield MM, Jovanovic S, et al. Mechanical unloading versus neurohumoral stimulation on myocardial structure and endocrine function In vivo. Circulation 2000;102:338–43.
41. Schena S, Kurimoto Y, Fukada J, et al. Effects of ventricular unloading on apoptosis and atrophy of cardiac myocytes. J Surg Res 2004;120: 119–26.
42. Campian ME, Verberne HJ, Hardziyenka M, et al. Serial noninvasive assessment of apoptosis during right ventricular disease progression in rats. J Nucl Med 2009;50:1371–7.
43. D'Armini AM, Zanotti G, Ghio S, et al. Reverse right ventricular remodeling after pulmonary endarterectomy. J Thorac Cardiovasc Surg 2007;133:162–8.
44. Campian ME, Hardziyenka M, Michel MC, Tan HL. How valid are animal models to evaluate treatments for pulmonary hypertension? Naunyn Schmiedebergs Arch Pharmacol 2006;373:391–400.

Key Words: atrophy ■ pulmonary hypertension ■ right ventricular failure.

APPENDIX

For an expanded Methods section, please see the online version of this article.